ADVANCES IN RADAR REMOTE SENSING OF WETLAND ECOSYSTEMS: COMBINATION OF SATELLITE OBSERVATIONS, FIELD DATA AND EM MODELS

H. Karszenbaum[(1)], P. Ferrazzoli[(2)] , F. M. Grings[(1)], , M. Salvia[(1)], P. Kandus[(3)], Pablo Perna[(1)]

(1) Instituto de Astronomía y Física del Espacio (IAFE), Ciudad Universitaria, 1428 Buenos Aires, República Argentina
(2) Università di Roma "Tor Vergata", Facoltà di Ingegneria, Dipartimento di Informatica, Sistemi e Produzione (DISP), Via del Politecnico 1, 00133 Roma, Italy
(3) Universidad de Buenos Aires, Facultad de Ciencias Exactas y Naturales (FCEyN), Dpto. de Ecología, Genética y Evolución, Laboratorio de Ecología Regional, Ciudad Universitaria, Pab. II, 1428 Buenos Aires, República Argentina,

Corresponding author:
P. Ferrazzoli
Email: ferrazzoli@disp.uniroma2.it

ABSTRACT

This paper focuses on the results obtained in the analysis of temporal series of ERS-2, RADARSAT-1 SAR and ENVISAT ASAR data acquired over wetland ecosystems of Argentina. The complete data set includes RADARSAT 1 images of 1997-98 that show an El Niño phenomenon, an ERS 2 temporal set covering 1999-2000 that shows the effect of burnt biomass and its recovery on the radar signature, and a temporal set of ASAR data which includes images acquired under different polarizations and incidence angles as well as different environmental conditions (water level, precipitation, and vegetation condition). Two marsh species, named *junco* and *cortadera,* were monitored. This overall data set is giving us the possibility of studying and understanding the basic interactions between the radar, the soil under different flood conditions, and the vegetation structure. The comprehension of the observed features was addressed through EM models development for these ecosystems.

1. INTRODUCTION

The Syntethic Aperture Radar (SAR) instrument is an active sensor onboard satellites that acquires data of the earth surface in the microwave region of the electromagnetic spectrum. In particular, in wetlands, it is capable of providing information about vegetation structure and hydrological conditions.

It is well documented that when standing water is present beneath the vegetation canopies, the radar response (backscattering coefficient, σ^0) changes depending on the dominant vegetation type, its density and height. Several authors have already reported on the characteristics of the backscattering coefficient σ^0 at various frequencies and polarizations for different types of wetland marshes. Among the most important, we can mention the works of [1], [2], and [3]. Reference [1] analyzed SIR-C polarimetric radar imagery of wetlands in Central America, and its main conclusions were that water under vegetation could be detected by an increase or a decrease of σ^0: increase in marshes with mainly vertical orientation, decrease in short, randomly oriented marshes. In the first case, the increase in HH is greater that in VV. Reference [2] reported comparable results analyzing the radar backscatter measured from ERS-2 imagery in Florida (USA) wetlands. In [3], the authors showed how it is possible to accurately delineate inundation and different vegetation types using multi-frequency polarimetric radar (SIR-C) along the Amazon floodplain.

This paper addresses a region of wetland marshes of Argentina which was observed by different SAR systems ([4], [5], [6] and [7]). Our purpose is to show how SAR instruments provide unique information regarding wetland structure and hydrology. Methodologically, our work is based on: i) multi-temporal and multi-polarization SAR data that address different environmental conditions in two types of marshes of different structure (*cortadera* and *junco*), ii) electromagnetic models that simulate the backscattering of these marshes and iii) field work corresponding to the acquisition dates.

An electromagnetic model is an algorithm that simulates the wetland radar response by obtaining the coefficient of backscattering σ^0 for vegetation and soil under different environmental conditions (flooded, non flooded, burn vegetation, others). Vegetation elements are modelled as simple objects (shoots as cylinders, leaves as disks). The model developed at Tor Vergata University is able to simulate the marsh σ^0 under various environmental conditions. By comparing simulated backscattering coefficients with experimental

ones, the electromagnetic model can be validated. Once the model is validated, it can be used, in conjunction to ground truth, to develop a retrieval scheme. In this way, the combination of observations, models and field work allows us to develop and test retrieval algorithms. (Example: an algorithm to monitor flood condition within marshes)

2. AREA DESCRIPTION

The Lower Delta of the Paraná River covers approximately 2,700 km^2. This area is a deltaic plain located at the terminal portion of De La Plata River basin. The Lower Delta hydrology is determined mainly by the Paraná River and the De La Plata estuary. The former has its main flood peak in the late-fall period. The second one has a moon and wind tide regime. The combination of local topographic gradients and a regional flooding regime constitutes the primary factor that determines the emergent natural vegetation. *Junco* and *cortadera* marshes cover the main portion of the region [5]. On the contrary, forests are restricted to levees and bars where soils are generally dry or flooded only during wind tides, and/or heavy fluvial floods. A large portion of the natural vegetation was replaced by *Salix* spp. and *Populus* spp. afforestation. Marshes cover up to 50% of the area, 20% of which are subjected to frequent fire events. Fires are intentional for wildlife hunting activities or just to prevent dried biomass accumulation. A dominant species of this type of marsh is *Schaenoplectus californicus*, a perennial equisetoid plant, up to 2.5 m tall growing in permanently flooded soils. This complex system not only shows seasonal variations but also annual and interannual fluctuations.

3. USES OF SARs IN THE PARANÁ RIVER WETLAND

Through different AO projects from the European Space Agency (ESA) and the Canadian Center of Remote Sensing (CCRS), several sets of SAR data were acquired over the wetland region addressed in this paper. Table 1 lists the data.

The following paragraphs describe the different applications that were developed using these data.

3.1 Wetland classification

Fig. 1 is a three polarizations image, obtained by joining S2 ASAR data with ERS-2 data on December 6, 2003, and amplifying the scale of HV. In the agricultural areas, VV is generally dominant, with some areas with relatively high HV, depending on crop type.

Table 1. Acquired SAR data

Satellite/instrument	Period	Comments
ERS-2/SAR, C band, VV polarization, single incidence angle	Temporal series 1999-2000 May 1998 November 2003 December 2000, 2003	various phenological and hydrological conditions.
RADARSAT/SAR, C band , HH polarization, different incidence angles	February, March and August , 1997 Two of May, 1998 Two of December, 2000	Flooded and non flooded conditions
ENVISAT/SAR,C band, APP mode for several incidence angles and combination of two of three polarizations HH, VV, and HV	Eight S1 scenes October 2003 to November 2005 Six S2 scenes, December 2003 to December 2005, Six S5 scenes, September 2003 to May 2004, Several S3, S4 and S6 scenes	various phenological and hydrological conditions.

The HV is higher in the forest areas in agreement with results of previous investigations. In both *junco* and *cortadera* marshes there is a clear dominance of HH. In order to give a quantitative picture of these discrimination properties, Fig. 2 shows a scatter plot built with mean values from polygons of four land covers types (*junco*, *cortadera*, forest and agriculture) extracted from the same image of Figure 1. In Fig. 2, the *x* axis indicates the ratios (in dB) between backscattering coefficients at HV and VV polarizations (HV-VV), and the *y* the ratios (in dB) between backscattering coefficients at HH and VV polarizations (HH-VV). The figure shows clusters corresponding to:

- Agricultural areas, where VV is slightly dominant over HH, and HV - VV is strongly negative (A in Fig.1).
- Forest, with values of HV - VV slightly negative and the HH - VV difference close to 0 dB (B in Fig.1).
- Junco marshes, with values of HV - VV slightly negative, and the HH - VV difference strongly positive (C in Fig.1).
- Cortadera marshes, where HV - VV is also slightly negative, and the HH - VV difference is moderately positive (D in Fig. 1).

This shows how different radar polarizations carry distinct information in wetlands.

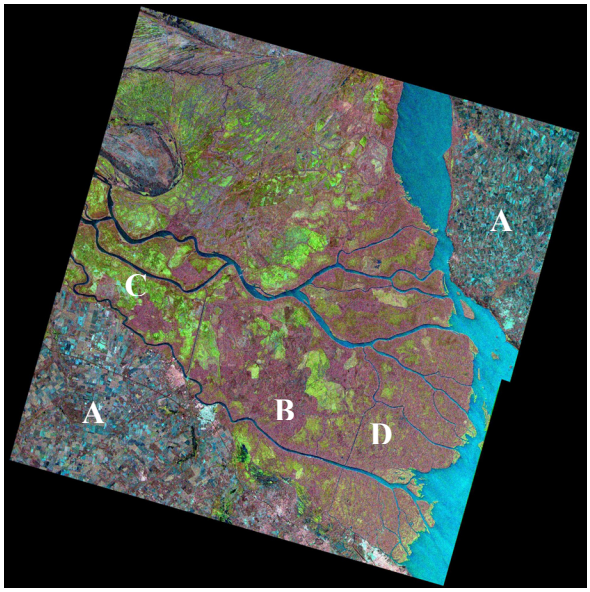

Fig. 1: An S2 (HV in red, HH in green) ASAR image combined with an ERS 2 SAR (VV, in blue)

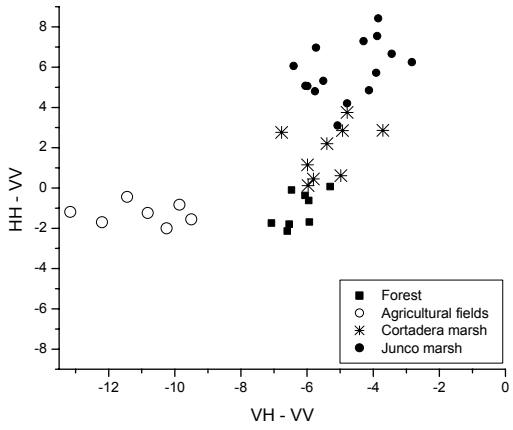

Fig. 2. Mean values scatter plot from polygons of four land covers (junco marsh, cortadera marsh, forest and agriculture) extracted from an image obtained by combining ENVISAT S2 ASAR data with ERS-2 data of the same day (6/Dec/2003). The x axis indicates the ratios (in dB) between backscattering coefficients at HV and VV polarizations (HV-VV), and the y axis indicates the ratios (in dB) between backscattering coefficients at HH and VV polarizations (HH-VV)

3.2 Modelling *junco* re-growth after burning

The Delta of the Paraná River was observed by ERS-2 SAR during years 1999-2000, which were characterized by a dry period followed by a wet period. From October 1999 to the end of the summer (March 2000), part of the *junco* marshes area suffered burning events, followed by re-growth. ERS-2 signatures proved to be able to monitor these events, showing an increase of σ^0 soon after burning, followed by a decrease observed during the phase of *junco* full development and senescence (See in Fig. 3, the *junco radar response* "bell-shape" trend). In order to explain this, we used an electromagnetic model that describes *junco* vegetation as a set of vertical dielectric cylinders on a flat flooded surface. Two main scattering sources were considered: double bounce between shoots and flooded soil, and ground. The electromagnetic model, together with the vegetation growth model, was used to predict the temporal evolution of the radar response during a burn-regrowth event. This simulation was compared with the ERS-2 VV data. The σ^0 "bell-shaped" temporal trend observed by ERS-2 was confirmed by the simulated data with a mean error of 2.5 dB. In this way, electromagnetic modeling results provide a sound theoretical interpretation of these observations [6].

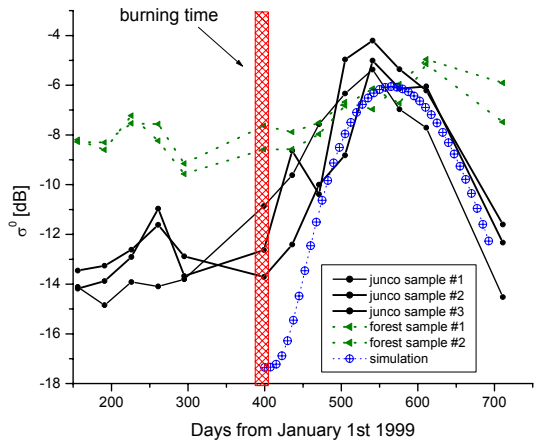

Fig. 3. Temporal trends of backscattering coefficients collected by ERS-2 over junco marshes and forests. (Adapted from [6])

3.3 Monitoring water level below marshes

In 20-Nov-03, the De la Plata river water level increased due to strong SE winds, and the Paraná River water level also increased. When this phenomenon happens, water from the river flows over the island levees and floods the *cortadera* and *junco* marsh. The flooding event in marshes does not last long, and by Apr-2004, the water level was in normal level again. ENVISAT ASAR observed the watershed during this event. To study this event, we have considered a multitemporal set of ASAR observations in Alternate Polarization mode (APP), at HH and VV polarization, at an angle of 19° (S1 configuration). Our objective

was to investigate the capability of a dual polarized C band radar to monitor marsh flooding. We have shown that when these marshes are flooded, the radar response increases significantly for both *cortadera* and *junco.* Figs. 4 and 5 show a multitemporal image that combines three different environmental conditions: in red the October image (spring and normal water levels in rivers), in green the November image (spring and a strong increase in water level) and in blue the March image (autumn starts). In VV polarization (Fig 4) the wetland radar response is quite uniform, and doesn't show multitemporal changes either. On the contrary, agricultural areas show a stronger response in the November image. In HH polarization (Fig 5) the wetland radar response shows important differences along the wetland area. On one hand, these are related to different vegetation covers. On the other, they are also due to temporal differences, which are related to distinct hydrological conditions at the acquisition time. These changes in the radar response can be attributed to the fact that the increase in water level reduces the amount of emerged biomass. Based on this, we proposed a vegetation-dependent flooding prediction scheme for two marsh structures: nearly vertical cylinders (*junco*-like) on flooded soils and randomly oriented discs (*cortadera*-like) also on flooded soils [7].

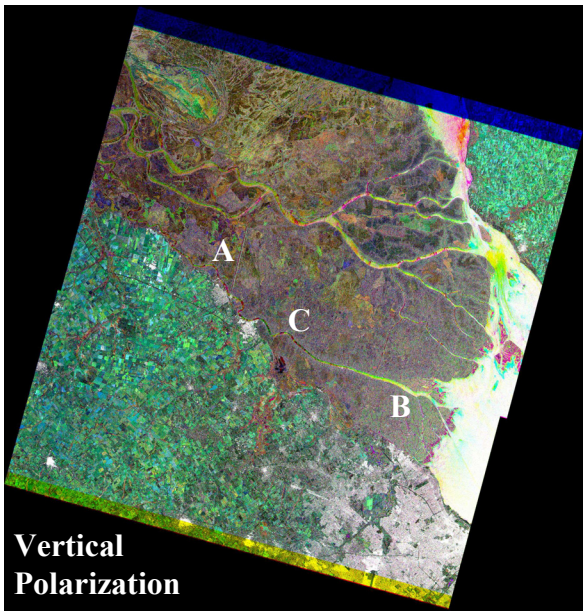

Fig. 4: S1 VV Multitemporal image (October, November, 2003, March 2004)

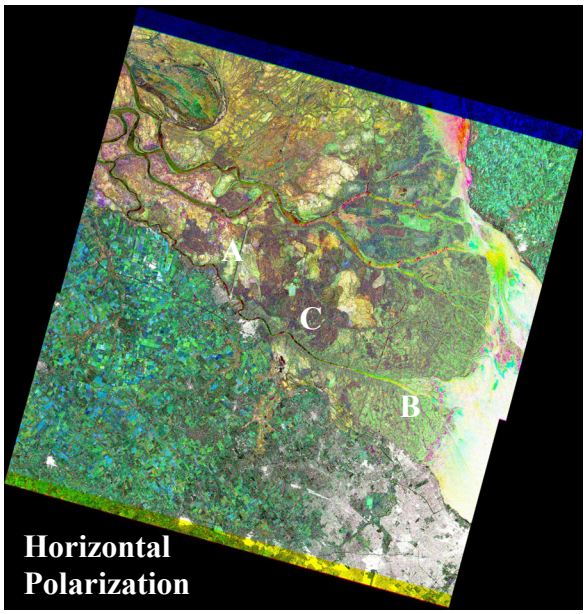

Fig. 5: S1 HH Multitemporal image (October, November, 2003, March 2004)

The effect of a decrease in the water level below the marshes is different in every polarization and every marsh. In the VV case (Fig. 6) it can be seen that σ^0 VV in the flooded condition is generally higher than σ^0 VV in the non-flooded condition for both marshes, but this change is marginal. Nevertheless the differences in HH polarization between flooded and non-flooded condition are much larger for both marshes (Fig. 7). This effect was already been observed by other authors on similar marshes [1][2].

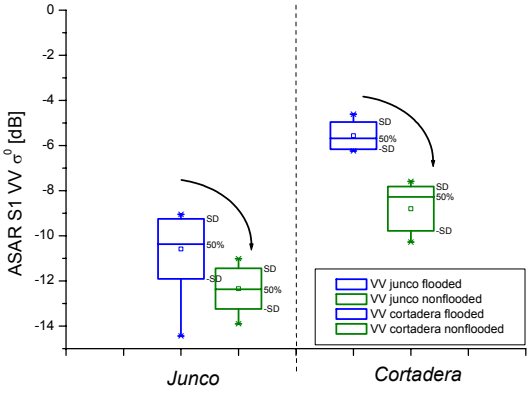

Fig. 6: Box plot diagrams resulting from ENVISAT data (VV polarization) collected over junco and cortadera marshes for two conditions (flooded: blue/non-flooded: green).

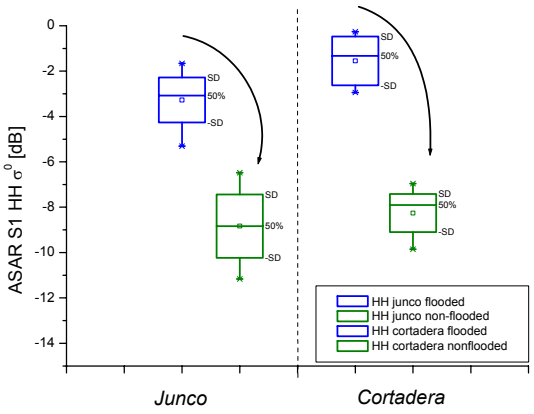

Fig. 7: Box plot diagrams resulting from ENVISAT data (HH polarization) collected over junco and cortadera marshes for two conditions (flooded: blue/non-flooded: green)

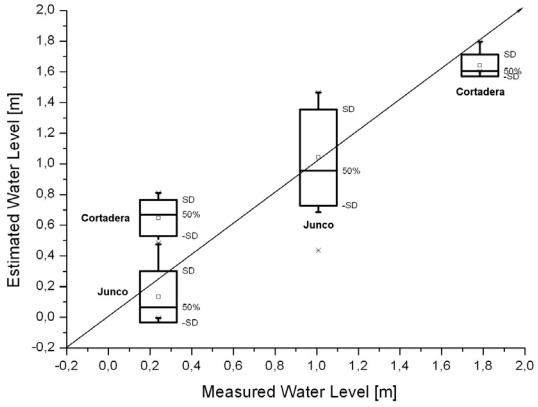

Fig. 8: Comparison between measured and estimated water level inside junco and cortadera marshes. The estimated water level was obtained by minimizing the Cost function (1)

4. WATER LEVEL RETRIEVAL SCHEME

For both November 20 and April 8 observations, an estimate of water level in *cortadera* and *junco* sites has been obtained with the aid of model simulations. This was done by finding the best estimation for a given set of ASAR dual polarization observations. Mathemathicaly, this is done by minimizing the Cost Function:

$$CF = \sum_{m=1}^{Ms} \sum_{p=1}^{2} \left[\sigma^0_{ppS}(WL) - \sigma^0_{ppEm} \right]^2 \qquad (1)$$

where $\sigma^0_{ppS}(WL)$ is the simulated backscattering coefficient at *pp* polarization for *WL* water level, σ^0_{ppEm} is the backscattering coefficient at the same polarization collected by ASAR over the marsh field and *Ms* is the number of marsh fields within the site. In the way it is stated, this algorithm chooses the WL that performs the best fit of HH and VV simultaneously.

Finally, estimated water levels have been compared with measured water levels. Results are shown in Fig. 8. For *junco* marshes and flooded *cortadera* marshes there is a general agreement. For non-flooded *cortadera* a systematic error is observed. This is due to a model underestimation of direct vegetation scattering from *cortadera* leaves. Indeed, *cortadera* leaves have a complex curved structure, which is only partially represented by the disc approximation.

The main objective of the work in progress is to investigate which are the conditions necessary to accurately estimate water level bellow marshes. Once the water level algorithm is developed and tested it could be used as an input for a hydrological process model. In fact, some papers show that the water inside the marshes located by the river sides can be used as a border condition to correct "pipe type" hydrological models. For the time being, the available data set is limited. Therefore, what we show is a first approach to the problem of quantitative water level retrieval inside marshes. Further refinements and validations will be possible after more data of present and future spaceborne SARs is collected.

5. FINAL REMARKS

Overall, results are promising, in view of future applications. However, further work aimed at improving the proposed technique is required. More ASAR measurements will allow us to consider a wider amount of water level conditions and higher angles. New extensive ground measurements will lead to a more detailed description of marsh structure. Also the addition of longer wavelengths could make the algorithm more reliable. Preliminary simulations indicated that the σ^0 trends vs. water level of an L band radar are appreciably different with respect to the C band case. For the time being, there are no experimental data to confirm these results, but the potential will be exploited in the future.

6. REFERENCES

1. Pope K. O., Rejmankova E., Paris F. F., Woodruff R., "Detecting seasonal flooding cicles in marshes of the Yucatan peninsula with SIR-C polarimetric radar imagery", Remote Sensing Environ. Vol. 59, pp. 157-166, 1997.
2. Kasischke E. S., Smith K. B., Bourgeau-Chavez L. L., Romanowicz E. A., Brunzell S., Richardson C. J., "Effects of the seasonal hydrologic patterns in South Florida wetlands on radar backsatter measured on ERS-2 SAR image," Remote Sensing Environ. Vol. 88, pp. 423-441, 2003.
3. Hess L. L, Melack J. M., Filoso S. and Wang Y., "Delineation of Inundated Area and Vegetation Along the Amazon Floodplain whit the SIR-C Synthetic Aperture Radar", *IEEE Transactions Geoscience and Remote Sensing*, Vol. 33, pp. 896-902, 1995
4. Parmuchi M. G., Karszenbaum H. and Kandus P., "Mapping the Paraná River delta wetland using multitemporal RADARSAT/SAR data and a decision based classifier". Canadian Journal of Remote Sensing, Vol. 28, pp. 631-635, 2002.
5. Karszenbaum H., Kandus P., Martinez J. M., Le Toan T., Tiffenberg J. and Parmuchi G., "ERS-2, RADARSAT SAR backscattering characteristics of the Paraná river delta wetlands, Argentina," ERS-Envisat Symposium (ESA), ESA-SP-461, 2000
6. Grings F. M., Ferrazzoli P., Karszenbaum H., Tiffenberg J., Kandus P., Guerriero L., Jacobo-Berlles J. C., "Modeling temporal evolution of *junco* marshes radar signatures", *IEEE Transactions Geoscience and Remote Sensing*, Vol. 43, pp. 2238-2245, 2005.
7. Grings F. M., Ferrazzoli P., Jacobo-Berlles J. C., Karszenbaum H., Tiffenberg J., Pratolongo P., Kandus P., "Monitoring flood condition in marshes using EM Models and ENVISAT ASAR observations", *IEEE Transactions Geoscience and Remote Sensing*, Vol. 44, pp. 936-942, 2006.